Original Article | Gastrointestinal Imaging

eISSN 2005-8330
https://doi.org/10.3348/kjr.2024.0980
Korean J Radiol 2025;26(4):346-359

Korean Journal of Radiology
KJR

Combination of CT/MRI LI-RADS With Second-Line Contrast-Enhanced Ultrasound Using Sulfur Hexafluoride or Perfluorobutane for Diagnosing Hepatocellular Carcinoma in High-Risk Patients

Yu Li[1]*, Sheng Li[2]*, Qing Li[1], Kai Li[3], Jing Han[1], Siyue Mao[2], Xiaohong Xu[4], Zhongzhen Su[5], Yanling Zuo[6], Shousong Xie[7], Hong Wen[8], Xuebin Zou[1], Jingxian Shen[2], Lingling Li[1], Jianhua Zhou[1]

[1]Department of Ultrasound, Sun Yat-sen University Cancer Center, State Key Laboratory of Oncology in South China, Collaborative Innovation Center for Cancer Medicine, Guangdong Provincial Clinical Research Center for Cancer, Guangzhou, China
[2]Department of Radiology, Sun Yat-sen University Cancer Center, State Key Laboratory of Oncology in South China, Collaborative Innovation Center for Cancer Medicine, Guangdong Provincial Clinical Research Center for Cancer, Guangzhou, China
[3]Department of Ultrasound, The Third Affiliated Hospital of Sun Yat-sen University, Guangzhou, China
[4]Department of Ultrasound, Affiliated Hospital of Guangdong Medical University, Zhanjiang, China
[5]Department of Ultrasound, The Fifth Affiliated Hospital of Sun Yat-sen University, Zhuhai, China
[6]Department of Ultrasound Imaging, Affiliated Cancer Hospital & Institute of Guangzhou Medical University, Guangzhou, China
[7]Department of Ultrasound, The First People's Hospital of Foshan, Foshan, China
[8]Department of Ultrasound, Huizhou Central People's Hospital, Huizhou, China

Objective: The CT/MRI Liver Imaging Reporting and Data System (LI-RADS) demonstrates high specificity with relatively limited sensitivity for diagnosing hepatocellular carcinoma (HCC) in high-risk patients. This study aimed to explore the possibility of improving sensitivity by combining CT/MRI LI-RADS v2018 with second-line contrast-enhanced ultrasound (CEUS) LI-RADS v2017 using sulfur hexafluoride (SHF) or perfluorobutane (PFB).

Materials and Methods: This retrospective analysis of prospectively collected multicenter data included high-risk patients with treatment-naive hepatic observations. The reference standard was pathological confirmation or a composite reference standard (only for benign lesions). Each participant underwent concurrent CT/MRI, SHF-enhanced US, and PFB-enhanced US examinations. The diagnostic performances for HCC of CT/MRI LI-RADS alone and three combination strategies (combining CT/MRI LI-RADS with either LI-RADS SHF, LI-RADS PFB, or a modified algorithm incorporating the Kupffer-phase findings for PFB [modified PFB]) were evaluated. For the three combination strategies, apart from the CT/MRI LR-5 criteria, HCC was diagnosed if CT/MRI LR-3 or LR-4 observations met the LR-5 criteria using LI-RADS SHF, LI-RADS PFB, or modified PFB.

Results: In total, 281 participants (237 males; mean age, 55 ± 11 years) with 306 observations (227 HCCs, 40 non-HCC malignancies, and 39 benign lesions) were included. Using LI-RADS SHF, LI-RADS PFB, and modified PFB, 20, 23, and 31 CT/MRI LR-3/4 observations, respectively, were reclassified as LR-5, and all were pathologically confirmed as HCCs. Compared to CT/MRI LI-RADS alone (74%, 95% confidence interval [CI]: 68%–79%), the three combination strategies combining CT/MRI LI-RADS with either LI-RADS SHF, LI-RADS PFB, or modified PFB increased sensitivity (83% [95% CI: 77%–87%], 84% [95% CI: 79%–

Received: September 2, 2024 **Revised:** November 11, 2024 **Accepted:** January 10, 2025
*These authors contributed equally to this work.
Corresponding author: Lingling Li, MD, Department of Ultrasound, Sun Yat-sen University Cancer Center, State Key Laboratory of Oncology in South China, Collaborative Innovation Center for Cancer Medicine, Guangdong Provincial Clinical Research Center for Cancer, No. 651 Dongfeng Road East, Guangzhou 510060, China
• E-mail: lill@sysucc.org.cn
Corresponding author: Jianhua Zhou, MD, PhD, Department of Ultrasound, Sun Yat-sen University Cancer Center, State Key Laboratory of Oncology in South China, Collaborative Innovation Center for Cancer Medicine, Guangdong Provincial Clinical Research Center for Cancer, No. 651 Dongfeng Road East, Guangzhou 510060, China
• E-mail: zhoujh@sysucc.org.cn

Korean Journal of Radiology
KJR

89%], 88% [95% CI: 83%–92%], respectively; all $P < 0.001$), while maintaining the specificity at 92% (95% CI: 84%–97%).
Conclusion: The combination of CT/MRI LI-RADS with second-line CEUS using SHF or PFB improved the sensitivity of HCC diagnosis without compromising specificity.
Keywords: Hepatocellular carcinoma; Liver imaging reporting and data system; Joint diagnosis; Contrast-enhanced ultrasound; Computed tomography; Magnet resonance imaging

INTRODUCTION

Hepatocellular carcinoma (HCC) can be noninvasively diagnosed by characteristic imaging findings without pathological confirmation in high-risk patients [1,2]. Contrast-enhanced CT/MRI is globally recognized as the first-line imaging modality for diagnosing HCC [3-6].

The CT/MRI Liver Imaging Reporting and Data System (LI-RADS) [7], a diagnostic algorithm that assigns a category for each observation in high-risk patients according to the likelihood of HCC, from the LR-1 category (definitely benign) to LR-5 category (definitely HCC), has been actively adopted in clinical practice [8-11]. High specificity for diagnosing HCC at the LR-5 level is essential for guiding treatment decisions without the need for biopsy confirmation. However, to maintain the high specificity of LR-5, its sensitivity is somewhat sacrificed [12]. Improving the sensitivity of HCC diagnosis at the LR-5 level would be beneficial for accurately identifying candidates for treatment and improving survival outcomes. High sensitivity for HCC is particularly important in regions where local therapeutic interventions are predominantly used instead of liver transplantation [7]. One factor contributing to the limited sensitivity of HCC could be the inherent limitations of CT/MRI in non-real-time examinations. Inaccurate arterial phase timing can fail to capture arterial phase hyperenhancement (APHE) in observations [13]. Among high-risk patients undergoing HCC surveillance, approximately 20% have liver lesions without APHE on CT/MRI [14]. These lesions, which present with some but not all hallmarks of HCC, are classified as LR-3 or LR-4 rather than LR-5. This underscores the necessity for immediate and effective problem-solving strategies to improve the sensitivity while preserving the specificity of the LR-5 category in HCC diagnosis.

Contrast-enhanced ultrasound (CEUS) with microbubbles, such as sulfur hexafluoride (SHF) and perfluorobutane (PFB), provides the advantage of real-time assessment of contrast enhancement, leading to superior sensitivity for detecting APHE compared to CT and MRI [5,13]. In previous studies, approximately 28% of lesions without APHE on CT/MRI presented with APHE on SHF-enhanced US [15]. PFB-enhanced US also detected APHE in approximately 29% of observations without APHE on CT/MRI [16]. Particular attention was paid to the role of the Kupffer phase in the PFB-enhanced US. PFB can be specifically phagocytosed by Kupffer cells in the liver, leading to persistent enhancement of normal liver parenchyma during the Kupffer phase. Lesions with a reduced number and function of Kupffer cells during hepatocarcinogenesis can manifest as Kupffer defect [5]. Kupffer-phase findings can assist in characterizing lesions without washout on MRI as HCC [17,18].

Therefore, a combination strategy combining CT/MRI and second-line CEUS may be beneficial for improving the diagnostic sensitivity for HCC without losing specificity. However, this has not been thoroughly explored. This study aimed to explore the possibility of improving sensitivity by combining CT/MRI LI-RADS with second-line CEUS with SHF or PFB.

MATERIALS AND METHODS

Participants

This study was a retrospective analysis of prospectively collected data. The study was approved by the local Institutional Review Board (IRB No. ChiCTR2100047035), which waived the requirement for informed consent.

A total of 375 high-risk patients with 424 treatment-naïve hepatic nodules detected by routine US screening or surveillance using contrast-enhanced CT or MRI from June 2021 to December 2021 were enrolled in a previous multicenter study [19]. All patients underwent SHF-enhanced and PFB-enhanced US on the same day. Patients also underwent concurrent CT and/or MRI examinations within 1 month. In the previous study, the CT/MRI LR-5 criteria were accepted for the noninvasive diagnosis of HCC in the absence of pathological confirmation. However, the diagnostic performance of CT/MRI LI-RADS as an index test for diagnosing HCC needs to be evaluated in the present study. To prevent CT/MRI from serving as both index tests and reference standards, 118 patients with 118 HCC lesions

 https://doi.org/10.3348/kjr.2024.0980

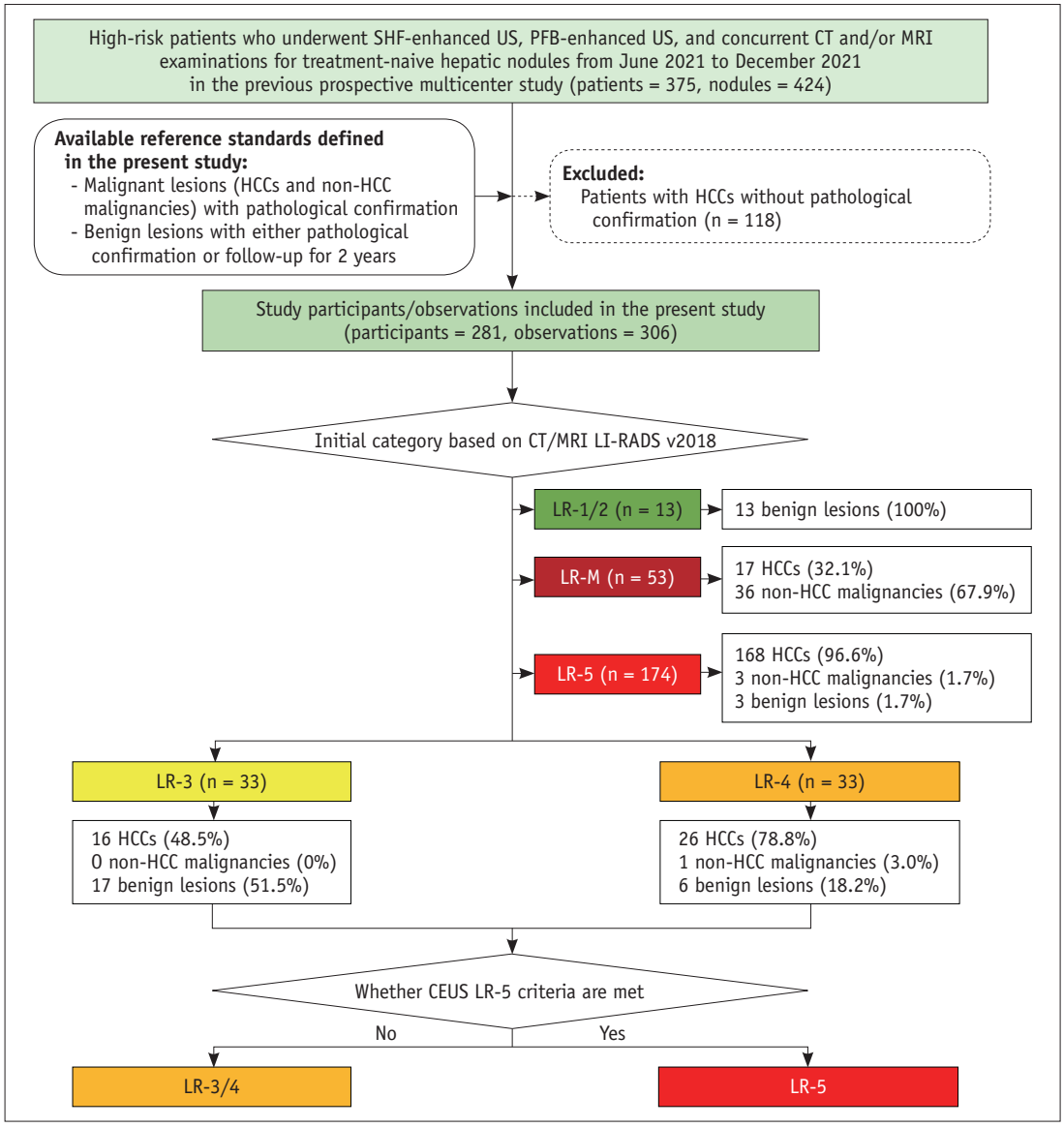

Fig. 1. Flow chart of study participants. SHF = sulfur hexafluoride, PFB = perfluorobutane, HCC = hepatocellular carcinoma, LI-RADS = Liver Imaging Reporting and Data System, CEUS = contrast-enhanced ultrasound

diagnosed by CT/MRI LR-5 criteria without pathological confirmation in the previous study were excluded. The remaining 281 participants with 306 observations with available reference standards (as described below) defined in the present study were finally included (Fig. 1).

CT and MRI Acquisition and Interpretation

In this study, 44 patients underwent contrast-enhanced CT only, 199 patients underwent contrast-enhanced MRI only, and 38 patients underwent both contrast-enhanced CT and contrast-enhanced MRI, as shown in Supplementary Table 1. Among 24 participants with more than one observation, only the three largest observations were included. CT examinations were performed using multiple multi-detector CT systems with iopromide (Ultravist, Bayer Schering Pharma, Berlin, Germany). MRI examinations were performed using a 1.5T or 3T system with either the extracellular agent gadopentetate dimeglumine (Magnevist, Bayer Schering Pharma) or the hepatobiliary agent gadoxetate disodium (Primovist, Bayer Schering Pharma). Details of the CT and MRI protocols are provided in Supplementary Materials 1.

Two readers (with 9 and 10 years of experience in abdominal imaging), who were blinded to the final diagnosis, laboratory results, medical records, and other imaging test results, independently reviewed all CT and MRI images. For each observation, the major features of HCC in

https://doi.org/10.3348/kjr.2024.0980

Korean Journal of Radiology
KJR

CT/MRI LI-RADS (non-rim APHE, non-peripheral washout, and enhancing capsule) and LR-M targetoid features were recorded. Disagreements were resolved by consultation with a third, more experienced reviewer (with 20 years of experience in abdominal imaging). For the 38 patients who underwent both CT and MRI examinations, the readers evaluated only the MRI findings, reflecting a more robust evaluation of certain LI-RADS features such as targetoid appearance on MRI. Each observation was assigned to a LI-RADS category in accordance with CT/MRI LI-RADS.

CEUS Acquisition and Interpretation

For each participant, grayscale, SHF-enhanced, and PFB-enhanced US were performed using multiple ultrasonic instruments. Contrast agents (for SHF-enhanced US: SonoVue, Bracco, Milan, Italy; for PFB-enhanced US: Sonazoid, GE Healthcare, Oslo, Norway) were administered. There was a minimum interval of 30 minutes between SHF-enhanced and PFB-enhanced US. Images were obtained in the vascular phase (i.e., arterial, portal venous, and late phases) and only for PFB-enhanced US in the Kupffer phase. Details of the CEUS protocols are provided in Supplementary Materials 2.

Two radiologists (with 13 and 12 years of experience in abdominal imaging, including liver CEUS), who were blinded to the final diagnosis, laboratory results, medical records, and other imaging test results, independently reviewed all SHF-enhanced US images in the first session and PFB-enhanced US images in the second session. There was a 1-month interval between the two sessions to avoid recall bias. For each observation, the features of APHE, washout time, and degree of washout were recorded on both SHF-enhanced US and PFB-enhanced US, and only for PFB-enhanced US, Kupffer defects. Disagreements were resolved by consultation with a third, more experienced reviewer (with 21 years of experience in abdominal imaging, including liver CEUS). Three LI-RADS categories were assigned to each observation: CEUS LI-RADS based on SHF-enhanced US (LI-RADS SHF), CEUS LI-RADS based on PFB-enhanced US (LI-RADS PFB), and a modified algorithm based on PFB-enhanced US (modified PFB). Compared to CEUS LI-RADS, the modified algorithm upgraded observations ≥10 mm with APHE, no washout, and a Kupffer defect from LR-4 to LR-5, and reassigned observations ≥10 mm with APHE, early washout, and mild Kupffer defect from LR-M to LR-5 [19].

Diagnostic Strategies

Four diagnostic strategies for HCC were evaluated: CT/MRI LI-RADS alone, and three combination strategies combining CT/MRI LI-RADS with either LI-RADS SHF, LI-RADS PFB, or modified PFB. Using CT/MRI LI-RADS alone, LR-5 assessed using CT or MRI was considered positive for the diagnosis of HCC. A two-step diagnostic process was implemented for combination strategies. First, HCC was diagnosed if an observation met the LR-5 criteria using CT/MRI LI-RADS (the same as CT/MRI LI-RADS alone). Second, HCC was diagnosed if LR-3 or LR-4 lesions on CT and MRI met the LR-5 criteria using either LI-RADS SHF, LI-RADS PFB, or modified PFB.

Reference Standard

Histological assessment (i.e., needle biopsy or surgical resection) of HCC and non-HCC malignancies was required. For benign lesions, either pathological confirmation or a composite reference standard was accepted as the reference standard. The composite standard for benign lesions was characteristic imaging features on CT or MRI, size reduction, or size stability during a minimum 2-year follow-up period.

Statistical Analysis

Continuous variables were presented as means and standard deviations, and categorical variables were presented as numbers and percentages. The inter-reader agreement for the binary categorization of LR-5 versus others was assessed by calculating Cohen's kappa (κ) coefficients with 95% confidence intervals [CIs], which were categorized as follows [20]: 0.00–0.20, slight agreement; 0.21–0.40, fair; 0.41–0.60, moderate; 0.61–0.80, substantial; and 0.81–1.00, excellent. Consensus interpretation of the imaging results was used to estimate diagnostic performance. The diagnostic performances of the four diagnostic strategies were assessed in terms of sensitivity, specificity, accuracy, positive predictive value (PPV), and negative predictive value. McNemar's test was used to compare the sensitivity, specificity, and accuracy of diagnostic strategies. $P < 0.013$ indicated a significant difference in the diagnostic performance results after Bonferroni correction for three pairwise comparisons. All statistical analyses were performed using SPSS (version 26.0, IBM Corp., Armonk, NY, USA). $P < 0.05$ indicated a significant difference unless otherwise stated.

RESULTS

Participant and Observation Characteristics

Finally, a total of 281 participants (237 males; mean age, 55 ± 11 years) with 306 observations (mean size, 40 ± 25 mm;

 https://doi.org/10.3348/kjr.2024.0980

Table 1. Characteristics of participants and observations

Characteristics	Values
Patients (n = 281)	
Age, yrs	55 ± 11 (24–86)
Sex	
Male	237 (84.3)
Female	44 (15.7)
Liver disease etiologic cause	
HBV	259 (92.2)
HCV	4 (1.4)
Alcohol	17 (6.0)
NAFLD	1 (0.4)
Presence of cirrhosis	169 (60.1)
History of HCC	32 (11.4)
Number of nodules per patient	
Single	257 (91.5)
Multiple	24 (8.5)
Observations (n = 306)	
Nodule size	40 ± 25 (7–153)
20 mm	71 (23.2)
>20 mm	235 (76.8)
Final diagnosis	
HCC	227 (74.2)
Non-HCC malignancy	
ICC	23 (7.5)
Combined HCC-ICC	4 (1.3)
Metastasis	10 (3.3)
Carcinosarcoma	1 (0.3)
Neuroendocrine neoplasm	1 (0.3)
Lymphoepithelioma-like carcinoma	1 (0.3)
Benign lesions	
Focal nodular hyperplasia	2 (0.7)
Regenerative or dysplastic nodule	17 (5.6)
Hemangioma	14 (4.6)
Solitary necrotizing nodule	1 (0.3)
Angiomyolipoma	2 (0.7)
Inflammatory pseudotumor	1 (0.3)
Benign, not specified	2 (0.7)
Reference standard	
HCC (n = 227)	
Pathologic confirmation	227 (100.0)
Surgical resection	167 (73.6)
Needle biopsy	60 (26.4)
Non-HCC malignancy (n = 40)	
Pathologic confirmation	40 (100.0)
Surgical resection	13 (32.5)
Needle biopsy	27 (67.5)
Benign lesion (n = 39)	
Pathologic confirmation	12 (30.8)
Surgical resection	4 (10.3)
Needle biopsy	8 (20.5)
Composite reference standard	27 (69.2)

Data are numbers of participants or nodules with percentages in parentheses, or mean ± standard deviation (range), unless indicated otherwise.
HBV = hepatitis B virus, HCV = hepatitis C virus, NAFLD = nonalcoholic fatty liver disease, HCC = hepatocellular carcinoma, ICC = intrahepatic cholangiocarcinoma

227 HCCs, 40 non-HCC malignancies, 39 benign lesions) were included. The clinicopathological characteristics of the study participants and their observations are summarized in Table 1. Among them, 71 of the 306 (23.2%) observations had a maximum diameter of less than 20 mm (hereafter referred to as small observations).

Imaging Features

Figure 2 presents the confusion matrices of the imaging features, and Table 2 provides an overview of the imaging features identified in the 227 HCC observations across various imaging modalities, including CT/MRI, SHF-enhanced US, and PFB-enhanced US. Non-rim APHE was observed in 81.5% (185/227) of HCCs on CT/MRI, whereas it was more frequently observed in 95.6% (217/227) and 96.0% (218/227) of HCCs on SHF-enhanced and PFB-enhanced US, respectively (both $P < 0.001$). Washout pattern was observed in 83.7% (190/227) of HCCs on CT/MRI, while it was observed in 80.2% (182/227, $P = 0.382$) and 82.8% (188/227, $P = 0.899$) of HCCs on SHF-enhanced US and PFB-enhanced US, respectively. A Kupffer defect on PFB-enhanced US was more frequently observed, in 94.7% (215/227) of HCCs, than the washout pattern on CT/MRI ($P < 0.001$).

The frequency and inter-reader agreement of imaging features on CT/MRI, SHF-enhanced US, and PFB-enhanced US for all 306 observations are summarized in Supplementary Tables 2 and 3, respectively.

Inter-Reader Agreement of Categorization as LR-5

Table 3 summarizes the inter-reader agreement for the binary categorization of LR-5 versus others. The κ values ranged 0.60–0.63, indicating moderate-to-substantial agreement.

LI-RADS Category Assignments

For all 306 observations, cross-tabulation of LI-RADS category assignments between CT/MRI LI-RADS paired with LI-RADS SHF, LI-RADS PFB, and modified PFB is shown in Figure 3, respectively. Using the CT/MRI LI-RADS, 13 (4.2%) observations were classified as LR-1 or LR-2, 33 (10.8%) as LR-3, 33 (10.8%) as LR-4, 174 (56.9%) as LR-5, and 53 (17.3%) as LR-M. Among the CT/MRI observations reclassified as LR-5 using LI-RADS SHF, LI-RADS PFB, and modified PFB (20, 23, and 31, respectively), 100% were pathologically confirmed as HCC.

For the 71 small observations, cross-tabulation of LI-RADS category assignments between CT/MRI LI-RADS paired with

https://doi.org/10.3348/kjr.2024.0980

Korean Journal of Radiology
KJR

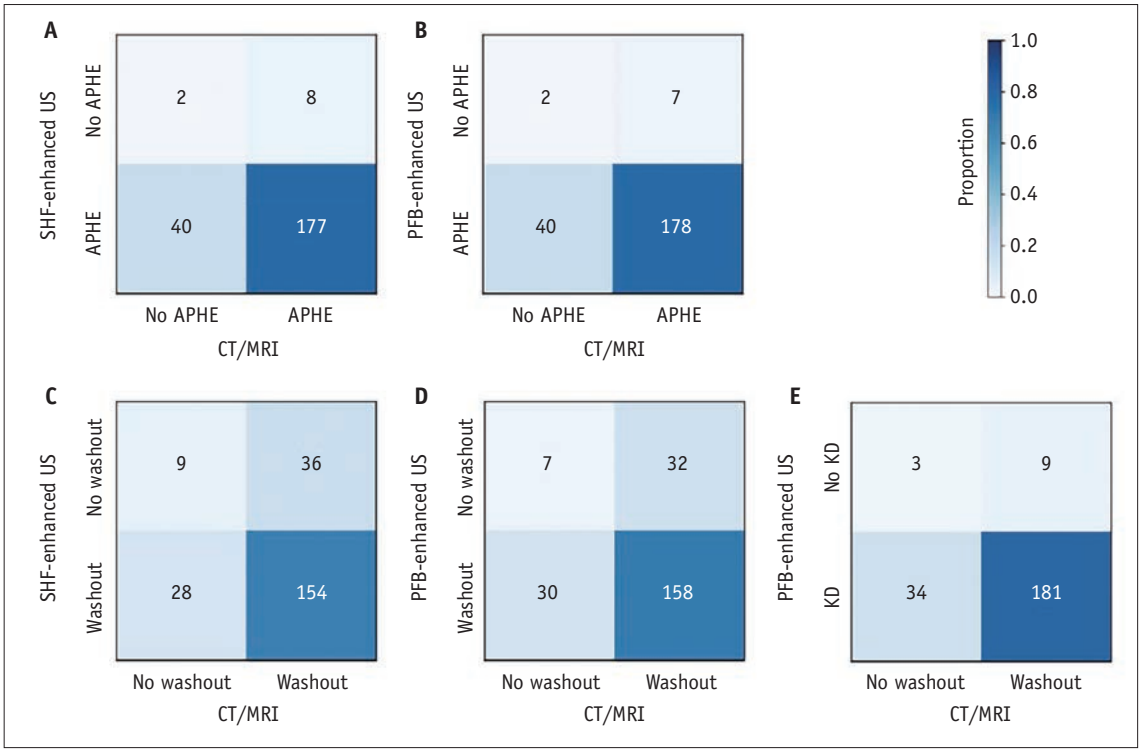

Fig. 2. Confusion matrices comparing imaging features between CT/MRI and contrast-enhanced US among 227 HCCs. **A-E:** Each matrix corresponds to a specific imaging feature. The value of each cell indicates the number of nodules. US = ultrasound, HCC = hepatocellular carcinoma, SHF = sulfur hexafluoride, APHE = arterial phase hyperenhancement, PFB = perfluorobutane, KD = Kupffer defect

Table 2. Summarize of imaging features on CT/MRI and contrast-enhanced US in 227 HCCs

Imaging features	Frequency	*P*
Nonrim APHE on CT/MRI	81.5 (185/227)	Reference*
Nonrim APHE on SHF-enhanced US	95.6 (217/227)	<0.001
Nonrim APHE on PFB-enhanced US	96.0 (218/227)	<0.001
Nonperipheral washout on CT/MRI	83.7 (190/227)	Reference*
Washout on SHF-enhanced US	80.2 (182/227)	0.382
Washout on PFB-enhanced US	82.8 (188/227)	0.899
Kupffer defect on PFB-enhanced US	94.7 (215/227)	<0.001

Data are percentages with numbers of nodules in parentheses.
**P*-value was frequency of imaging features on contrast-enhanced US compared with those on CT/MRI. $P < 0.05$ indicated a significant difference.
US = ultrasound, HCC = hepatocellular carcinoma, APHE = arterial phase hyperenhancement, SHF = sulfur hexafluoride, PFB = perfluorobutane

LI-RADS SHF, LI-RADS PFB, and modified PFB are shown in Figure 4, respectively. Using the CT/MRI LI-RADS, 4 (5.6%) small observations were classified as LR-1 or LR-2, 24 (33.8%) as LR-3, 6 (8.5%) as LR-4, 28 (39.4%) as LR-5, and 9 (12.7%) as LR-M. Among the small observations reclassified as LR-5 using the LI-RADS SHF, LI-RADS PFB, and modified PFB (7, 6, and 10, respectively), 100% were pathologically confirmed as HCC.

Table 3. Inter-reader agreement for binary categorization as LR-5 vs. others

Methods	κ value (95% CI)
CT/MRI LI-RADS	0.63 (0.56–0.70)
LI-RADS SHF	0.60 (0.53–0.67)
LI-RADS PFB	0.60 (0.52–0.67)
Modified PFB	0.61 (0.54–0.68)

CI = confidence interval, LI-RADS = Liver Imaging Reporting and Data System, SHF = sulfur hexafluoride, PFB = perfluorobutane

Example images of two pathologically confirmed HCCs assigned LR-3 by CT/MRI LI-RADS but LR-5 by LI-RADS SHF, LI-RADS PFB, and modified PFB, are provided in Figure 5 and Figure 6, respectively. Example images of pathologically confirmed HCC assigned as LR-3 by CT/MRI LI-RADS, LR-4 by both LI-RADS SHF and LI-RADS PFB, and LR-5 by modified PFB are provided in Supplementary Figure 1.

Diagnostic Performance of Different Diagnostic Strategies

Table 4 shows the diagnostic performance of the CT/MRI LI-RADS alone and the three combination strategies combining the CT/MRI LI-RADS with LI-RADS SHF, LI-RADS PFB, or modified PFB. For all 306 observations, CT/MRI LI-

https://doi.org/10.3348/kjr.2024.0980

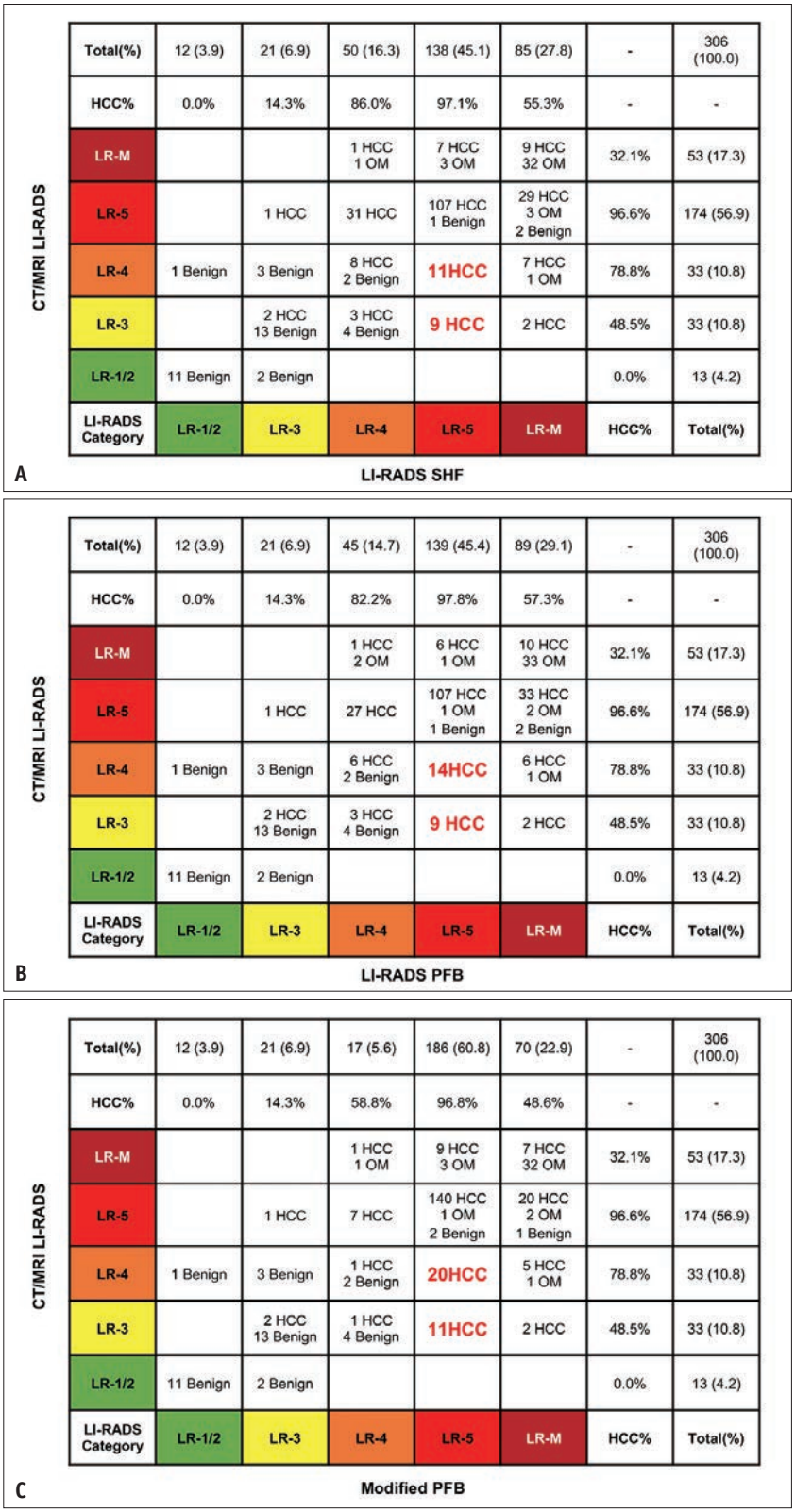

A

CT/MRI LI-RADS	LR-1/2	LR-3	LR-4	LR-5	LR-M	HCC%	Total(%)
Total(%)	12 (3.9)	21 (6.9)	50 (16.3)	138 (45.1)	85 (27.8)	-	306 (100.0)
HCC%	0.0%	14.3%	86.0%	97.1%	55.3%	-	-
LR-M			1 HCC 1 OM	7 HCC 3 OM	9 HCC 32 OM	32.1%	53 (17.3)
LR-5		1 HCC	31 HCC	107 HCC 1 Benign	29 HCC 3 OM 2 Benign	96.6%	174 (56.9)
LR-4	1 Benign	3 Benign	8 HCC 2 Benign	11HCC	7 HCC 1 OM	78.8%	33 (10.8)
LR-3		2 HCC 13 Benign	3 HCC 4 Benign	9 HCC	2 HCC	48.5%	33 (10.8)
LR-1/2	11 Benign	2 Benign				0.0%	13 (4.2)
LI-RADS Category	LR-1/2	LR-3	LR-4	LR-5	LR-M	HCC%	Total(%)

LI-RADS SHF

B

CT/MRI LI-RADS	LR-1/2	LR-3	LR-4	LR-5	LR-M	HCC%	Total(%)
Total(%)	12 (3.9)	21 (6.9)	45 (14.7)	139 (45.4)	89 (29.1)	-	306 (100.0)
HCC%	0.0%	14.3%	82.2%	97.8%	57.3%	-	-
LR-M			1 HCC 2 OM	6 HCC 1 OM	10 HCC 33 OM	32.1%	53 (17.3)
LR-5		1 HCC	27 HCC	107 HCC 1 OM 1 Benign	33 HCC 2 OM 2 Benign	96.6%	174 (56.9)
LR-4	1 Benign	3 Benign	6 HCC 2 Benign	14HCC	6 HCC 1 OM	78.8%	33 (10.8)
LR-3		2 HCC 13 Benign	3 HCC 4 Benign	9 HCC	2 HCC	48.5%	33 (10.8)
LR-1/2	11 Benign	2 Benign				0.0%	13 (4.2)
LI-RADS Category	LR-1/2	LR-3	LR-4	LR-5	LR-M	HCC%	Total(%)

LI-RADS PFB

C

CT/MRI LI-RADS	LR-1/2	LR-3	LR-4	LR-5	LR-M	HCC%	Total(%)
Total(%)	12 (3.9)	21 (6.9)	17 (5.6)	186 (60.8)	70 (22.9)	-	306 (100.0)
HCC%	0.0%	14.3%	58.8%	96.8%	48.6%	-	-
LR-M			1 HCC 1 OM	9 HCC 3 OM	7 HCC 32 OM	32.1%	53 (17.3)
LR-5		1 HCC	7 HCC	140 HCC 1 OM 2 Benign	20 HCC 2 OM 1 Benign	96.6%	174 (56.9)
LR-4	1 Benign	3 Benign	1 HCC 2 Benign	20HCC	5 HCC 1 OM	78.8%	33 (10.8)
LR-3		2 HCC 13 Benign	1 HCC 4 Benign	11HCC	2 HCC	48.5%	33 (10.8)
LR-1/2	11 Benign	2 Benign				0.0%	13 (4.2)
LI-RADS Category	LR-1/2	LR-3	LR-4	LR-5	LR-M	HCC%	Total(%)

Modified PFB

Fig. 3. Cross-tabulation of LI-RADS category assignments between CT/MRI LI-RADS paired with **(A)** LI-RADS SHF, **(B)** LI-RADS PFB, and **(C)** modified PFB for all 306 observations. Of 66 observations assessed as LR-3 or LR-4 by CT/MRI LI-RADS alone, 20 (30.3%), 23 (34.8%), and 31 (47.0%) were characterized as LR-5 using LI-RADS SHF, LI-RADS PFB, and modified PFB, respectively (100% HCC). LI-RADS = Liver Imaging Reporting and Data System, SHF = sulfur hexafluoride, PFB = perfluorobutane, HCC = hepatocellular carcinoma, OM = non-HCC malignancy

https://doi.org/10.3348/kjr.2024.0980

Korean Journal of Radiology
KJR

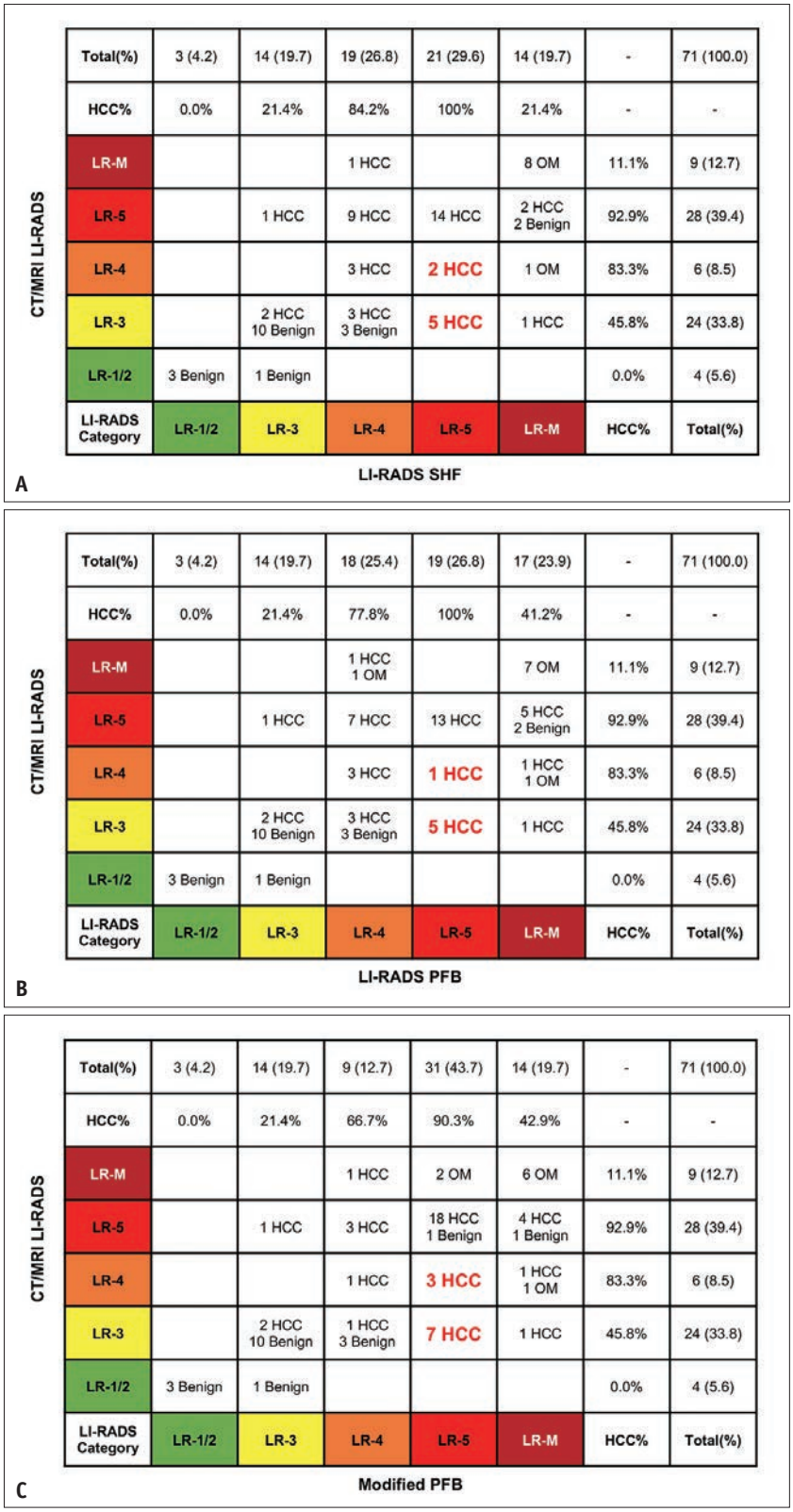

A

CT/MRI LI-RADS	LR-1/2	LR-3	LR-4	LR-5	LR-M	HCC%	Total(%)
Total(%)	3 (4.2)	14 (19.7)	19 (26.8)	21 (29.6)	14 (19.7)	-	71 (100.0)
HCC%	0.0%	21.4%	84.2%	100%	21.4%	-	-
LR-M			1 HCC		8 OM	11.1%	9 (12.7)
LR-5		1 HCC	9 HCC	14 HCC	2 HCC 2 Benign	92.9%	28 (39.4)
LR-4			3 HCC	2 HCC	1 OM	83.3%	6 (8.5)
LR-3		2 HCC 10 Benign	3 HCC 3 Benign	5 HCC	1 HCC	45.8%	24 (33.8)
LR-1/2	3 Benign	1 Benign				0.0%	4 (5.6)
LI-RADS Category	LR-1/2	LR-3	LR-4	LR-5	LR-M	HCC%	Total(%)

LI-RADS SHF

B

CT/MRI LI-RADS	LR-1/2	LR-3	LR-4	LR-5	LR-M	HCC%	Total(%)
Total(%)	3 (4.2)	14 (19.7)	18 (25.4)	19 (26.8)	17 (23.9)	-	71 (100.0)
HCC%	0.0%	21.4%	77.8%	100%	41.2%	-	-
LR-M			1 HCC 1 OM		7 OM	11.1%	9 (12.7)
LR-5		1 HCC	7 HCC	13 HCC	5 HCC 2 Benign	92.9%	28 (39.4)
LR-4			3 HCC	1 HCC	1 HCC 1 OM	83.3%	6 (8.5)
LR-3		2 HCC 10 Benign	3 HCC 3 Benign	5 HCC	1 HCC	45.8%	24 (33.8)
LR-1/2	3 Benign	1 Benign				0.0%	4 (5.6)
LI-RADS Category	LR-1/2	LR-3	LR-4	LR-5	LR-M	HCC%	Total(%)

LI-RADS PFB

C

CT/MRI LI-RADS	LR-1/2	LR-3	LR-4	LR-5	LR-M	HCC%	Total(%)
Total(%)	3 (4.2)	14 (19.7)	9 (12.7)	31 (43.7)	14 (19.7)	-	71 (100.0)
HCC%	0.0%	21.4%	66.7%	90.3%	42.9%	-	-
LR-M			1 HCC	2 OM	6 OM	11.1%	9 (12.7)
LR-5		1 HCC	3 HCC	18 HCC 1 Benign	4 HCC 1 Benign	92.9%	28 (39.4)
LR-4			1 HCC	3 HCC	1 HCC 1 OM	83.3%	6 (8.5)
LR-3		2 HCC 10 Benign	1 HCC 3 Benign	7 HCC	1 HCC	45.8%	24 (33.8)
LR-1/2	3 Benign	1 Benign				0.0%	4 (5.6)
LI-RADS Category	LR-1/2	LR-3	LR-4	LR-5	LR-M	HCC%	Total(%)

Modified PFB

Fig. 4. Cross-tabulation of LI-RADS category assignments between CT/MRI LI-RADS paired with **(A)** LI-RADS SHF, **(B)** LI-RADS PFB, and **(C)** modified PFB for 71 observations with a maximum diameter of less than 20 mm. Of 30 small observations assessed as LR-3 or LR-4 by CT/MRI LI-RADS, 7 (23.3%), 6 (20.0%), and 10 (33.3%) were characterized as LR-5 using LI-RADS SHF, LI-RADS PFB, and modified PFB, respectively (100% HCC). LI-RADS = Liver Imaging Reporting and Data System, SHF = sulfur hexafluoride, PFB = perfluorobutane, HCC = hepatocellular carcinoma, OM = non-HCC malignancy

https://doi.org/10.3348/kjr.2024.0980

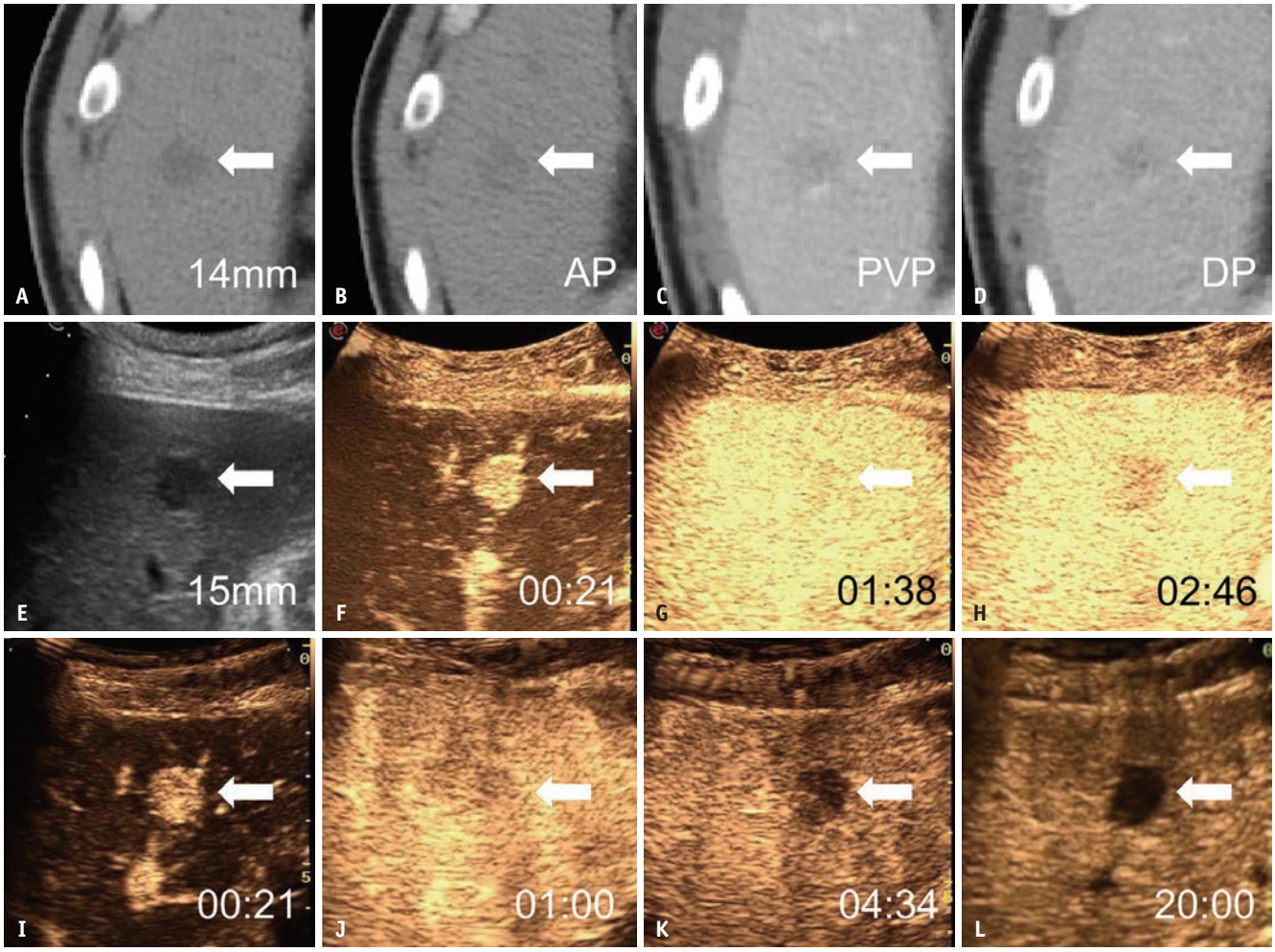

Fig. 5. Images of a 39-year-old male at high risk of HCC due to chronic hepatitis B virus infection. **A:** On contrast-enhanced CT with iopromide, plain image shows a 14 mm hypodensity observation in segment VI (arrow). **B:** AP image showing the absence of non-rim APHE (arrow). **C, D:** PVP and DP images show non-peripheral washout (arrows). **E:** Grayscale US image showing a 15 mm hypoechoic observation in segment VI (arrow). **F:** On SHF-enhanced US, the AP image at 21 seconds shows non-rim APHE (arrow). **G:** Portal venous-phase image at 1:38 minutes shows no washout (arrow). **H:** Late-phase image at 2:46 minutes showing late and mild washout (arrow). **I:** On PFB-enhanced US, the AP image at 21 seconds shows non-rim APHE (arrow). **J:** PVP image at 1 minute showing no washout (arrow). **K:** Late-phase image at 4:34 minutes showing late and mild washout (arrow). **L:** Kupffer-phase image at 20 minutes shows a marked Kupffer defect (arrow). This observation was assigned as LR-3 by CT/MRI LI-RADS and LR-5 according to the following criteria: LI-RADS SHF, LI-RADS PFB, and modified PFB. The pathological diagnosis based on the needle biopsy was HCC. HCC = hepatocellular carcinoma, AP = arterial phase, APHE = arterial hyperenhancement, PVP = portal venous-phase, DP = delayed-phase, US = ultrasound, SHF = sulfur hexafluoride, PFB = perfluorobutane, LI-RADS = Liver Imaging Reporting and Data System

RADS alone yielded a sensitivity of 74% (95% CI: 68%, 79%), specificity of 92% (95% CI: 84%, 97%), accuracy of 79% (95% CI: 74%, 83%), and PPV of 97% (95% CI: 92%, 99%) for diagnosing HCC. Compared to CT/MRI LI-RADS alone, the combination strategies combining CT/MRI LI-RADS with LI-RADS SHF had increased sensitivity (83%, 95% CI: 77%, 87%, $P < 0.001$) and increased accuracy (85%, 95% CI: 81%, 89%, $P < 0.001$) without losing PPV (97%, 95% CI: 93%, 99%); with PFB had increased sensitivity (84%, 95% CI: 79%, 89%, $P < 0.001$) and increased accuracy (86%, 95% CI: 82%, 90%, $P < 0.001$) without losing PPV (97%, 95% CI: 93%, 99%); with modified PFB had increased sensitivity (88%, 95% CI: 83%, 92%; $P < 0.001$) and increased accuracy (89%, 95% CI: 85%, 92%, $P < 0.001$) without losing PPV (97%, 95% CI: 93%, 99%). The same specificity (92%, 95% CI: 84%, 97%) was achieved for all four diagnostic strategies.

For 71 small observations, CT/MRI LI-RADS alone yielded a sensitivity of 60% (95% CI: 44%, 75%), specificity of 93% (95% CI: 75%, 99%), accuracy of 73% (95% CI: 62%,

https://doi.org/10.3348/kjr.2024.0980

Korean Journal of Radiology
KJR

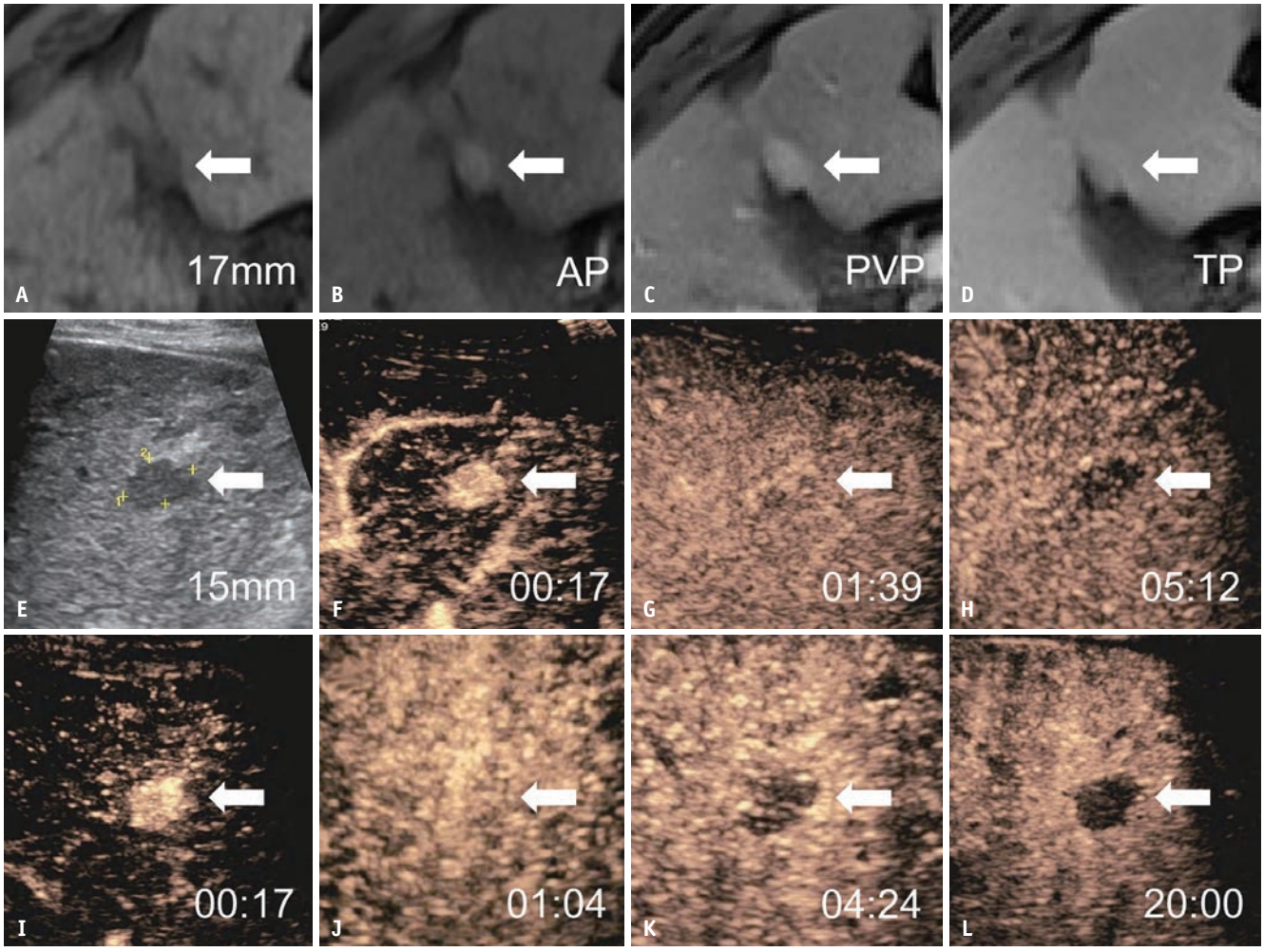

Fig. 6. Images of a 52-year-old male at high risk of HCC due to liver cirrhosis caused by chronic hepatitis B virus infection. **A:** On contrast-enhanced MRI with hepatobiliary agent gadoxetate disodium, T1-weighted image shows a 17 mm hypointense observation in segment IV/V (arrow). **B:** AP image shows non-rim APHE (arrow). **C:** PVP image shows the observation without non-peripheral washout (arrow). **D:** TP image shows the observation without enhancing "capsule" (arrow). **E:** Gray-scale US image showing a 15 mm hypoechoic observation in segments IV/V (arrow and calipers 1 and 2). **F:** On SHF-enhanced US, the AP image at 17 seconds shows non-rim APHE (arrow). **G:** PVP image at 1:39 minutes showing no washout (arrow). **H:** Late-phase image at 5:12 minutes showing late and mild washout (arrow). **I:** On PFB-enhanced US, AP image at 17 seconds shows non-rim APHE (arrow). **J:** PVP image at 1:04 minutes showing no washout (arrow). **K:** Late-phase image at 4:24 minutes showing late and mild washout (arrow). **L:** Kupffer-phase image at 20 minutes shows a marked Kupffer defect (arrow). This observation was assigned as LR-3 by CT/MRI LI-RADS and LR-5 according to the following criteria: LI-RADS SHF, LI-RADS PFB, and modified PFB. The pathological diagnosis based on the needle biopsy was HCC. HCC = hepatocellular carcinoma, AP = arterial phase, APHE = arterial hyperenhancement, PVP = portal venous-phase, TP = transitional-phase, US = ultrasound, SHF = sulfur hexafluoride, PFB = perfluorobutane, LI-RADS = Liver Imaging Reporting and Data System

82%), and PPV of 93% (95% CI: 75%, 99%) for diagnosing HCC. Compared to CT/MRI LI-RADS alone, the combination strategies combining CT/MRI LI-RADS with LI-RADS SHF and LI-RADS PFB showed no evidence of a statistically significant difference in sensitivity (77% [95% CI: 61%, 88%], $P = 0.016$ and 74% [95% CI: 59%, 86%], $P = 0.031$, respectively) or accuracy (83% [95% CI: 73%, 90%], $P = 0.016$ and 82% [95% CI: 71%, 89%], $P = 0.031$, respectively) without losing PPV (94%, [95% CI: 79%, 99%], for both), and with modified PFB had increased sensitivity (84%, 95% CI: 69%, 93%, $P = 0.002$) and increased accuracy (87%, 95% CI: 78%, 93%, $P = 0.002$) without losing PPV (95%, 95% CI: 81%, 99%). The same specificity (93%, 95% CI: 75%, 99%) was achieved for all four diagnostic strategies.

DISCUSSION

This study aimed to explore the possibility of improving the

https://doi.org/10.3348/kjr.2024.0980

Table 4. Diagnostic performance of different criteria for the diagnosis of HCC

Diagnostic strategy	Sensitivity	*P*	Specificity	*P*	Accuracy	*P*	PPV	NPV
All observations (n = 306)								
1. CT/MRI LI-RADS	74 (68–79) [168/227]	-	92 (84–97) [73/79]	-	79 (74–83) [241/306]	-	97 (92–99) [168/174]	55 (46–64) [73/132]
2. CT/MRI LI-RADS + LI-RADS SHF	83 (77–87) [188/227]	<0.001*	92 (84–97) [73/79]	N/A	85 (81–89) [261/306]	<0.001*	97 (93–99) [188/194]	65 (56–74) [73/112]
3. CT/MRI LI-RADS + LI-RADS PFB	84 (79–89) [191/227]	<0.001*	92 (84–97) [73/79]	N/A	86 (82–90) [264/306]	<0.001*	97 (93–99) [191/197]	67 (57–76) [73/109]
4. CT/MRI LI-RADS + modified PFB	88 (83–92) [199/227]	<0.001*	92 (84–97) [73/79]	N/A	89 (85–92) [272/306]	<0.001*	97 (93–99) [199/205]	72 (62–80) [73/101]
Observations with a maximum diameter of less than 20 mm (n = 71)								
1. CT/MRI LI-RADS	60 (44–75) [26/43]	-	93 (75–99) [26/28]	-	73 (62–82) [52/71]	-	93 (75–99) [26/28]	60 (44–75) [26/43]
2. CT/MRI LI-RADS + LI-RADS SHF	77 (61–88) [33/43]	0.016	93 (75–99) [26/28]	N/A	83 (73–90) [59/71]	0.016	94 (79–99) [33/35]	72 (55–85) [26/36]
3. CT/MRI LI-RADS + LI-RADS PFB	74 (59–86) [32/43]	0.031	93 (75–99) [26/28]	N/A	82 (71–89) [58/71]	0.031	94 (79–99) [32/34]	70 (53–84) [26/37]
4. CT/MRI LI-RADS + modified PFB	84 (69–93) [36/43]	0.002*	93 (75–99) [26/28]	N/A	87 (78–93) [62/71]	0.002*	95 (81–99) [36/38]	79 (61–90) [26/33]

Data are percentages with 95% confidence intervals in parentheses and raw numbers of nodules in brackets.
*$P < 0.013$ indicated a significant difference after Bonferroni correction for three pairwise comparisons against CT/MRI LI-RADS.
HCC = hepatocellular carcinoma, PPV = positive predictive value, NPV = negative predictive value, LI-RADS = Liver Imaging Reporting and Data System, SHF = sulfur hexafluoride, PFB = perfluorobutane

sensitivity in diagnosing HCC at the LR-5 level while preserving specificity by combining CT/MRI LI-RADS with second-line CEUS using either SHF or PFB. Among the CT/MRI observations reclassified as LR-5 using the LI-RADS SHF, LI-RADS PFB, and modified PFB (20, 23, and 31, respectively), 100% were pathologically confirmed as HCC. Compared to CT/MRI LI-RADS alone (74%), the three combination strategies combining CT/MRI LI-RADS with either LI-RADS SHF, LI-RADS PFB, or modified PFB showed increased sensitivity (83%, 84%, and 88%, respectively; all $P < 0.001$) without sacrificing specificity (92% for all).

In this study, LI-RADS category assignments between CT/MRI LI-RADS paired with LI-RADS SHF, LI-RADS PFB, and modified PFB showed many inconsistencies, which was consistent with a previous study [21]. Although the CEUS LI-RADS shares similar concepts of the LI-RADS category with the CT/MRI LI-RADS, there are several differences between the diagnostic algorithms, reflecting dissimilarities in the methods of image acquisition and types of contrast agents [22]. These two modalities provide distinct, yet probably complementary, information. This might explain why the cross-tabulation showed many inconsistencies.

CEUS allows real-time assessment of contrast enhancement of an observation, which virtually eliminates the possibility of arterial phase mistiming and can detect APHE in approximately 28% of observations without APHE on CT or MRI [15,16]. Similar results were obtained in this study; greater proportions of APHE were observed on CEUS than on CT/MRI (CT/MRI: 81.5%, SHF-enhanced US: 95.6%, PFB-enhanced US: 96.0%; both $P < 0.001$). In addition, PFB-enhanced US allows additional evaluation of lesions in the Kupffer phase. In the present study, a washout pattern on CT/MRI was observed in 83.7% of HCCs, whereas 94.7% of HCCs demonstrated a Kupffer defect on PFB-enhanced US ($P < 0.001$). In agreement with the results of this study, according to a Korean study, 30.8% of LR-3 and 62.2% of LR-4 HCC lesions in the absence of washout on MRI presented as Kupffer defects in the Kupffer phase [17]. Based on the LI-RADS, APHE and washout are important imaging features of the LR-5 categorization for diagnosing HCC; LR-5 cannot be assigned to lesions lacking APHE and washout on CT and MRI. In this case, CEUS is a reasonable problem-solving modality for improving the sensitivity of the LR-5 category in HCC diagnosis by detecting APHE or Kupffer defects without APHE or washout on CT and MRI.

Observations with some but not all hallmarks of HCC are classified as LR-3 or LR-4, which are considered indeterminate findings, to maintain the high specificity of

https://doi.org/10.3348/kjr.2024.0980

Korean Journal of Radiology
KJR

LR-5 for diagnosing HCC. Indeterminate results are commonly observed in high-risk patients undergoing HCC surveillance [14]. Although biopsy is not routinely recommended because of associated risks such as bleeding and tumor seeding, delayed follow-up imaging may lead to delayed treatment of HCC and increased clinical and financial burdens [3-6,23]. Reclassification of CT/MRI as LR-3 and LR-4 using second-line CEUS could achieve further stratification of the probability of HCC. In this study, among the CT/MRI observations reclassified as LR-5 using LI-RADS SHF, LI-RADS PFB, and modified PFB (20, 23, and 31, respectively), 100% were pathologically confirmed as HCC. This might be attributed to high specificity and high PPV of LR-5 for diagnosing HCC using these three CEUS algorithms [19,24-26]. Based on these findings, we suggest that HCC can be diagnosed if LR-3 or LR-4 lesions on CT and MRI meet the LR-5 criteria on second-line CEUS. Measures should be taken to ensure timely treatment of patients with LR-5 lesions on second-line CEUS instead of follow-up imaging.

In a previous study on SHF and PFB, both contrast agents used in enhanced US showed very high specificity for HCC, but low sensitivity [27]. However, high sensitivity for HCC, particularly early-stage HCC, will be beneficial in identifying candidates for treatment and improving survival. Therefore, it is crucial in regions that rely primarily on local treatments instead of transplantation. Enhancing the sensitivity of the LR-5 category for diagnosing HCC, while maintaining high specificity, has been pursued. In this study, compared to the CT/MRI LI-RADS alone (74%), the three combination strategies combining the CT/MRI LI-RADS with second-line CEUS had increased sensitivity (83%, 84%, and 88% for LI-RADS SHF, LI-RADS PFB, and modified PFB, respectively; All $P < 0.001$) without sacrificing specificity (92% for all) for all observations. The combination strategy of the CT/MRI LI-RADS with second-line CEUS has the potential to meet these unmet clinical needs.

The present study has several limitations. First, owing to the exploratory post hoc nature of this study, a potential bias, albeit unclear, might be involved. Second, data were collected from a population predominantly infected with the hepatitis B virus, and the generalizability of these findings remains unclear. Third, this study did not address the correlation or clustering of multiple lesions in the same patient. Finally, the analytical results for small observations with a maximum diameter of less than 20 mm were based on a small sample and thus need to be viewed with caution.

In conclusion, the combination of the CT/MRI LI-RADS with second-line CEUS using SHF or PFB improved the sensitivity of HCC diagnosis without compromising specificity.

Supplement

The Supplement is available with this article at https://doi.org/10.3348/kjr.2024.0980.

Availability of Data and Material

Data generated or analyzed during the study are available from the corresponding author by request.

Conflicts of Interest

The authors have no potential conflicts of interest to disclose.

Author Contributions

Conceptualization: Yu Li, Sheng Li, Lingling Li, Jianhua Zhou. Data curation: Kai Li, Xiaohong Xu, Zhongzhen Su, Yanling Zuo, Shousong Xie, Hong Wen. Fomal analysis: Yu Li, Lingling Li. Funding acquisition: Jianhua Zhou. Investigation: Sheng Li, Qing Li, Siyue Mao, Jing Han, Xuebin Zou, Jingxian Shen, Jianhua Zhou. Methodology: Yu Li, Sheng Li, Lingling Li, Jianhua Zhou. Project administration: Lingling Li, Jianhua Zhou. Supervision: Lingling Li, Jianhua Zhou. Validation: Sheng Li. Writing—original draft: Yu Li, Sheng Li. Writing—review & editing: all authors.

ORCID IDs

Yu Li
https://orcid.org/0000-0001-6935-6353
Sheng Li
https://orcid.org/0000-0003-1419-3475
Qing Li
https://orcid.org/0000-0002-8632-9637
Kai Li
https://orcid.org/0000-0003-3982-494X
Jing Han
https://orcid.org/0000-0003-3187-1397
Siyue Mao
https://orcid.org/0000-0003-0337-3673
Xiaohong Xu
https://orcid.org/0000-0002-3860-9845
Zhongzhen Su
https://orcid.org/0000-0002-7281-7357
Yanling Zuo
https://orcid.org/0009-0000-7457-104X

Shousong Xie
https://orcid.org/0009-0003-6619-8363
Hong Wen
https://orcid.org/0009-0007-5638-9923
Xuebin Zou
https://orcid.org/0000-0002-3484-9673
Jingxian Shen
https://orcid.org/0000-0002-9233-2576
Lingling Li
https://orcid.org/0000-0003-4596-8712
Jianhua Zhou
https://orcid.org/0000-0003-2096-8126

Funding Statement

This study was supported by National Natural Science Foundation of China (No. 82320108011).

REFERENCES

1. Marrero JA, Kulik LM, Sirlin CB, Zhu AX, Finn RS, Abecassis MM, et al. Diagnosis, staging, and management of hepatocellular carcinoma: 2018 practice guidance by the American Association for the Study of Liver Diseases. *Hepatology* 2018;68:723-750
2. Cassinotto C, Aubé C, Dohan A. Diagnosis of hepatocellular carcinoma: an update on international guidelines. *Diagn Interv Imaging* 2017;98:379-391
3. Singal AG, Llovet JM, Yarchoan M, Mehta N, Heimbach JK, Dawson LA, et al. AASLD practice guidance on prevention, diagnosis, and treatment of hepatocellular carcinoma. *Hepatology* 2023;78:1922-1965
4. European Association for the Study of the Liver. EASL clinical practice guidelines: management of hepatocellular carcinoma. *J Hepatol* 2018;69:182-236
5. Omata M, Cheng AL, Kokudo N, Kudo M, Lee JM, Jia J, et al. Asia-Pacific clinical practice guidelines on the management of hepatocellular carcinoma: a 2017 update. *Hepatol Int* 2017;11:317-370
6. Korean Liver Cancer Association (KLCA), National Cancer Center (NCC) Korea. 2022 KLCA-NCC Korea practice guidelines for the management of hepatocellular carcinoma. *Korean J Radiol* 2022;23:1126-1240
7. Chernyak V, Fowler KJ, Kamaya A, Kielar AZ, Elsayes KM, Bashir MR, et al. Liver imaging reporting and data system (LI-RADS) version 2018: imaging of hepatocellular carcinoma in at-risk patients. *Radiology* 2018;289:816-830
8. van der Pol CB, Lim CS, Sirlin CB, McGrath TA, Salameh JP, Bashir MR, et al. Accuracy of the liver imaging reporting and data system in computed tomography and magnetic resonance image analysis of hepatocellular carcinoma or overall malignancy-a systematic review. *Gastroenterology* 2019;156:976-986
9. Yoon JH, Kim YK, Kim JW, Chang W, Choi JI, Park BJ, et al. Comparison of four diagnostic guidelines for hepatocellular carcinoma using gadoxetic acid–enhanced liver MRI. *Radiology* 2024;311:e233114
10. Kwag M, Choi SH, Choi SJ, Byun JH, Won HJ, Shin YM. Simplified LI-RADS for hepatocellular carcinoma diagnosis at gadoxetic acid-enhanced MRI. *Radiology* 2022;305:614-622
11. Min JH, Kim JM, Kim YK, Kang TW, Lee SJ, Choi GS, et al. Prospective intraindividual comparison of magnetic resonance imaging with gadoxetic acid and extracellular contrast for diagnosis of hepatocellular carcinomas using the liver imaging reporting and data system. *Hepatology* 2018;68:2254-2266
12. Kanneganti M, Singal AG. Diagnosis and management of indeterminate liver nodules in patients with cirrhosis. *Clin Liver Dis (Hoboken)* 2023;22:181-183
13. Takahashi M, Maruyama H, Shimada T, Kamezaki H, Sekimoto T, Kanai F, et al. Characterization of hepatic lesions (≤ 30 mm) with liver-specific contrast agents: a comparison between ultrasound and magnetic resonance imaging. *Eur J Radiol* 2013;82:75-84
14. Konerman MA, Verma A, Zhao B, Singal AG, Lok AS, Parikh ND. Frequency and outcomes of abnormal imaging in patients with cirrhosis enrolled in a hepatocellular carcinoma surveillance program. *Liver Transpl* 2019;25:369-379
15. Kang HJ, Kim JH, Joo I, Han JK. Additional value of contrast-enhanced ultrasound (CEUS) on arterial phase non-hyperenhancement observations (≥2 cm) of CT/MRI for high-risk patients: focusing on the CT/MRI LI-RADS categories LR-3 and LR-4. *Abdom Radiol (NY)* 2020;45:55-63
16. Mandai M, Koda M, Matono T, Nagahara T, Sugihara T, Ueki M, et al. Assessment of hepatocellular carcinoma by contrast-enhanced ultrasound with perfluorobutane microbubbles: comparison with dynamic CT. *Br J Radiol* 2011;84:499-507
17. Kim YY, Min JH, Hwang JA, Jeong WK, Sinn DH, Lim HK. Second-line Sonazoid-enhanced ultrasonography for liver imaging reporting and data system category 3 and 4 on gadoxetate-enhanced magnetic resonance imaging. *Ultrasonography* 2022;41:519-529
18. Jeong WK, Kang HJ, Choi SH, Park MS, Yu MH, Kim B, et al. Diagnosing hepatocellular carcinoma using Sonazoid contrast-enhanced ultrasonography: 2023 guidelines from the Korean Society of Radiology and the Korean Society of Abdominal Radiology. *Korean J Radiol* 2023;24:482-497
19. Li L, Zou X, Zheng W, Li Y, Xu X, Li K, et al. Contrast-enhanced US with sulfur hexafluoride and perfluorobutane: LI-RADS for diagnosing hepatocellular carcinoma. *Radiology* 2023;308:e230150
20. Landis JR, Koch GG. The measurement of observer agreement for categorical data. *Biometrics* 1977;33:159-174
21. Ding J, Long L, Zhang X, Chen C, Zhou H, Zhou Y, et al. Contrast-enhanced ultrasound LI-RADS 2017: comparison with CT/MRI LI-RADS. *Eur Radiol* 2021;31:847-854
22. Kim TK, Noh SY, Wilson SR, Kono Y, Piscaglia F, Jang HJ, et al.

Contrast-enhanced ultrasound (CEUS) liver imaging reporting and data system (LI-RADS) 2017 - a review of important differences compared to the CT/MRI system. *Clin Mol Hepatol* 2017;23:280-289
23. Nahon P, Layese R, Ganne-Carrié N, Moins C, N'Kontchou G, Chaffaut C, et al. The clinical and financial burden of nonhepatocellular carcinoma focal lesions detected during the surveillance of patients with cirrhosis. *Hepatology* 2024;79:813-828
24. Zheng W, Li Q, Zou XB, Wang JW, Han F, Li F, et al. Evaluation of contrast-enhanced US LI-RADS version 2017: application on 2020 liver nodules in patients with hepatitis B infection. *Radiology* 2020;294:299-307
25. Terzi E, Iavarone M, Pompili M, Veronese L, Cabibbo G, Fraquelli M, et al. Contrast ultrasound LI-RADS LR-5 identifies hepatocellular carcinoma in cirrhosis in a multicenter restropective study of 1,006 nodules. *J Hepatol* 2018;68:485-492
26. Li L, Zheng W, Wang J, Han J, Guo Z, Hu Y, et al. Contrast-enhanced ultrasound using perfluorobutane: impact of proposed modified LI-RADS criteria on hepatocellular carcinoma detection. *AJR Am J Roentgenol* 2022;219:434-443
27. Kang HJ, Lee JM, Yoon JH, Yoo J, Choi Y, Joo I, et al. Sonazoid™ versus SonoVue® for diagnosing hepatocellular carcinoma using contrast-enhanced ultrasound in at-risk individuals: a prospective, single-center, intraindividual, noninferiority study. *Korean J Radiol* 2022;23:1067-1077

 https://doi.org/10.3348/kjr.2024.0980